sciendo

Chloroquine degradation in aqueous solution under electron beam irradiation

Stephen Kabasa [ID],
Yongxia Sun [ID],
Sylwester Bułka [ID],
Andrzej G. Chmielewski [ID]

Abstract. Pharmaceutically active compounds are the most widely produced and consumed consumer products that pose a substantial threat to the environment and living organisms owing to their pharmacokinetics, side effects, and contraindications. In this study, the degradation of chloroquine (CQ), a popular antimalarial and recently proposed COVID-19 drug, was investigated under electron beam (EB) irradiation of aqueous solutions. Both the hydroxyl radical and hydrated electron generated in the radiolysis of water contribute to the degradation of CQ in aqueous solution. The overall removal efficiency for 125 mg·L^{-1} of the CQ solution under EB treatment is reported to be >80% at neutral pH at a maximum irradiation dose of 7 kGy. Removal efficiency is further favored by acidic and slightly alkaline conditions where reactions with hydroxyl radicals and hydrated electrons are favored, respectively. Additionally, increments in the applied dose resulted in the increased removal efficiency for the same concentration of CQ. Conversely, the removal efficiency decreased with increasing concentration of CQ at the same irradiation dose. The initial solution pH, applied irradiation dose, and initial pollutant concentration play an important role in the EB-induced degradation of CQ by influencing the available oxidizing and reducing species. The chemical oxygen demand (COD) and total organic carbon (TOC) were not significantly decreased during the treatment process and indicated the formation of organic byproducts, which were not further degraded under the current experimental conditions.

Keywords: Advanced oxidation processes • Aqueous solution • Chloroquine • Degradation • Electron beam

Introduction

Industrial and domestic discharge of active pharmaceutical ingredients into the environment is inadequately regulated worldwide. The implications of these compounds, when present in water, soil, and air, to both plants and animals cannot be overlooked [1–3]. Repurposing wastewater effluents to serve as a source of irrigation water for the cultivation of food crops poses insurmountable risks. Antibiotics negatively affect the growth of food crops and affect the soil biota [4–7]. They tend to accumulate in plant roots and shoots and pose a threat to the food chain [8]. Similarly, pharmaceutical-degradation products and metabolites due to their lipophilic property, high toxicity, and resistance to degradation are of great concern [9, 10]. Wastewater can be classified by the presence of pathogens and physicochemical constituents that pose a risk to human and environmental health. Economical, efficient, and environmentally friendly treatment technolo-

S. Kabasa [✉], Y. Sun, S. Bułka, A. G. Chmielewski
Institute of Nuclear Chemistry and Technology
Dorodna 16 St., 03-195 Warsaw, Poland
E-mail: s.kabasa@ichtj.waw.pl

gies to remove these constituents are imperative in addressing these concerns [11, 12]. Moreover, detecting these contaminants in the ambient environment is paramount [13–15]. These compounds classified as emerging pollutants (EPs) are directly injected from industries, institutions, and sewage effluents. Electron beam technology is efficient for wastewater treatment and addresses the shortfalls of conventional wastewater treatment. It has shown efficacy for a myriad of emerging organic compounds of pollution concern.

Chloroquine (CQ) and hydroxychloroquine (HCQ) piqued interest as proposed therapeutics for severe acute respiratory syndrome coronavirus 2 (*SARS*CoV2) that causes COVID-19. CQ, a 4-aminoquinoline, is commonly used as a substitute for quinine in antimalarial therapy [1]. It is excreted unchanged or as metabolites via the kidney and feces as 3-hydroxyquinine and N-desethyl chloroquine [16] and enters the aquatic environment or is absorbed by the soil [17]. Quinoline derivatives are recalcitrant, persistent, toxic, carcinogenic, and teratogenic and therefore might pose a potential threat to living organisms and the environment due to their transport, transfer, and fate in the water environment based on their chemical stability [18].

Previous works on the degradation and removal of CQ from aqueous solutions mainly involved photostability studies, advanced oxidative processes (AOP) with or without catalysts, and adsorption technologies. Catalytic processes involving ferrate--Fe(VI) show CQ aromatic ring dealkylation and chloride ion substitution under the influence of pH, temperature, HCO_3^-, and humic acids with subsequent reduction in antimicrobial activity toward *Escherichia coli* and intermediates toxicity [19]. Catalytic wet air oxidation (CWAO) also degrades CQ phosphate simulated wastewater under anaerobic and aerobic conditions [11]. In addition, electro--Fenton processes (EFPs) using a boron-doped diamond anode have achieved (>90%) organic carbon removal [20–22]. The sulfate radical-advanced oxidation process (SR-AOP) utilizing $SO_4^{\cdot-}$ (E = 2.5–3.1 V) also degrades CQ under acidic conditions [23]. Similarly, biomass carbon-based catalysts also efficiently degrade CQ in a wide pH range (3–11) [24, 25], and the biochar-supported red mud catalyst (RM-BC) activated persulfate process degrades CQ phosphate, HCQ sulfate, and other COVID-19 drugs [26]. Specialized activated carbon sorbents manufactured from palm kernel (*Elaeis guineensis*) [27] and plantain peel-activated carbon-supported zinc oxide (PPAC-ZnO) [28] possess CQ adsorption capacity. Similarly, agar–graphene oxide (A-GO) hydrogel, granular activated carbon–graphene oxide (GAC-GO) [29, 30], biochar [31], and organo-clay kaolinite treated with citric acid [32] adsorb CQ with high efficiency (Table 1). Membranes are also a widely used option for removing pollutants from water. *E. coli* engineered to express tyrosinase enzyme on the surface have been used to produce the biopolymer melanin [42]. A membrane bioreactor for the removal of CQ has been developed with low pH regeneration releasing all the CQ without ap-

parent capacity loss over three consecutive cycles [33]. Most of these methods employ a phase transfer of the pollutant without destroying it. Additionally, these methods require the use of additives that require further processing to remove their byproducts. The electron beam processing does not require additives and destroys pollutants by reactions involving hydroxyl radicals and hydrated electrons. In this work, CQ degradation in aqueous solution under electron beam irradiation has been investigated.

Methodology

Materials

CQ phosphate powder (98.5–100.0%), potassium dichromate (99%), silver nitrate (99%), sodium hydroxide (99%), sulfuric acid (95%), and perchloric acid (95%) were purchased from Sigma-Aldrich (Merck, Germany). Distilled water from a Thermo Fischer scientific distillation unit (Merck, Germany) was used in the preparation of all solutions for this study.

Analytical techniques

The Jasco-V670 UV-VIS (Poland) and Macherey Nagel Nanocolor VIS II (Germany) spectrophotometers were used for the detection of CQ (>1 mg·L^{-1}) at the maximum absorption wavelength of 343 nm. Nanocolor test kits produced by Macherey Nagel (Germany) were purchased from Aqua Labs (Poland) for photometric determination of total Kjeldahl nitrogen (TKN) (1.0–16 mg·L^{-1}), total nitrogen (0.5–50 mg·L^{-1}), nitrate NO_3^-, NH_4^+ (0.2–8 mg·L^{-1}), Cl$^-$ (0.5–50 mg·L^{-1}), total organic carbon (TOC) (20–300 mg·L^{-1}), and chemical oxygen demand (COD) (50–300 mg·L^{-1}). Photometric tests were performed using the Nanocolor VIS II spectrophotometer. The pH measurements were conducted using an Elemetron CX-461 multimeter (Poland). Dissolved oxygen (DO) was measured using a DO meter from Mettler Toledo (Poland).

Radiation processing

Radiation processing was done in batch mode. The aqueous solutions containing different CQ concentrations were prepared in distilled water. Irradiation was performed on the ILU6 accelerator at an energy of 1.65 MeV, 2 Hz, and 50 mA. Potassium dichromate (0.0005 M) solution in perchloric acid with silver nitrate and alanine dosimeters were used to assess the applied doses ranging from 0.5 kGy to 7 kGy [43–46]. Low-density polyethylene (LDPE) sleeve bags were filled with 35 mL of CQ solution and irradiated under the accelerator window. The initial pH values of the CQ solution were adjusted with 0.1 M NaOH and 0.1 M H_2SO_4 to study the effect of pH on the degradation efficiency under electron beam processing.

Table 1. Methods previously used for the removal of CQ from aqueous solutions

Methods	Conditions	Removal efficiency	Ref.
Membranes			
Membrane bioreactors – tyrosinase enzyme on *Escherichia coli* biopolymer	pH 7.5, 20 h	98% with 140 ± 6 mg·g^{-1} No apparent capacity loss over three consecutive cycles	[33]
Adsorbents			
Activated carbon Palm kernel (*Elaeis guineensis*) shells		Large surface areas, strong mechanical characteristics	[27]
PPAC-ZnO	313 K 10 ppm CQ	78.89% Adsorption capacity increases with temperature	[28]
A-GO hydrogel		Adsorption 63 mg·g^{-1}	[29, 30]
GAC-GO	Equilibrium time 18 h	37.65 mg·g^{-1} Adsorption	
Organo-clay raw kaolinite treated with citric acid	20 mg·L^{-1} CQ 120 min	99.28% Maximum sorption capacity is 4.03 mg·g^{-1}	[32]
Soybean hull residues functionalized with iron oxide nanoparticles (SBH-Fe$_3$O$_4$)	120 min 318 K	Adsorption capacity 98.84 mg·g^{-1} Reuse five cycles	[34]
Iron and magnesium comodified rape straw biochar (Fe/Mg-RSB)	pH (3–11) CQ 4–25 mg·L^{-1} at 180 r·min^{-1} for 8 h 308 K	Adsorption capacity of 42.93 mg·g^{-1}	[35]
MOF sheet, namely BUC-21(Fe) FeSO$_4$·7H$_2$O, 1,3-dibenzyl-2-imidazoli-done-4,5-dicarboxylic acid (H$_2$L) and 4,4′-bipyridine (bpy)	pH = 5.0 30 min	100% $C_{\cdot OH}$ 242.5 mmol·L^{-1}, H$_2$O$_2$ consumption 83.2%	[36]
Catalysts			
Ferrate-Fe(VI)	CQ 10 μM Fe(VI) 40–180 mM time 1–20 min	59% CQ removal Algae, antimicrobial, toxicity reduction	[19]
CWAO HEO – (MgCuMnCoFe) Ox	Oxygen pressure of 15 bar, catalyst dosage of 1.4 g·L^{-1}, and temperature of 230°C	34.6% and 41.2% higher than that without the HEO system	[11]
Single cobalt atoms in a defined Co–N$_3$ coordination structure	pH range (3–11) employing the SA Co-N-C (30)	100%	[24, 25]
Biochar-supported RM-BC activated persulfate process	20 mg·L^{-1} 40 min	84.8%	[26]
Carbon nanotube-loaded CoFe$_2$O$_4$ (CoFe$_2$O$_4$@CNTs) composite	10 mg·L^{-1} CQ pH 7	Mineralization efficiency 33%, removal efficiency 98.7%	[37]
Advanced oxidation processes			
SR-AOP	Peroxymonosulfate (PMS, HSO$_5^-$) peroxy disulfate (PDS, S$_2$O$_8^{2-}$) 10.0 mg·L^{-1}	P25M175-94.6% within 30 min	[23]
UV/PS	pH = 6.9 10 min	91.3% CQ reactions with ·OH and SO$_4^{\cdot-}$ were 8.9×10^9 L·(mol·s)$^{-1}$ and 1.4×10^{10} L·(mol·s)$^{-1}$	[38]
Photocatalysis-activated SR-AOP over PDINH/MIL-88A(Fe) composites	10.0 mg·L^{-1} CQ P25M175 30 min	94.6% Good reusability and stability	[23]

Table 1. *continued*

Methods	Conditions	Removal efficiency	Ref.
Electrocoagulation	66.89 mA·cm⁻², 600 rpm 60 min electrolysis time 3 mg·L⁻¹ CQ, pH = 6.5	95% dissolved aluminum electrodes 0.228 kg·m⁻³ energy consumption of 12.243 kWh·m⁻³	[39]
EFP	Carbon felt cathode and BDD anode	92% (TOC)	[20]
FBER	BDD electrodes batch recirculation mode 9 h, pH 5.38, 34.4 mA·cm⁻², and liquid flow rate (Q) of 1.42 L·min⁻¹	Degradation 89.3%, COD 51.6%, mineralization 53.1% energy consumption 0.041 kWh·L⁻¹	[40]
Electro-Fenton with pyrite (FeS₂)-modified graphite felt (FeS₂/GF) cathode	pH of 3.0 FeS₂ loading-10 mg, current density 150 mA, electrode spacing 2.0 cm	83.3 ± 0.4% 60 min CQ removal, retains 60.0% CQ removal in consecutive batch tests	[41]

A-GO, agar-graphene oxide; BDD, boron-doped diamond; CQ, chloroquine; CWAO, catalytic wet air oxidation; EFP, electro--Fenton processes; FBER, flow-by electrochemical reactor; GAC-GO, granular activated carbon–graphene oxide; HEO, high entropy oxide; PPAC-ZnO, plantain peel-activated carbon-supported zinc oxide; RM-BC, red mud catalyst; SR-AOP, sulfate radical-advanced oxidation process; TOC; total organic carbon; UV/PS, UV-activated persulfate system; PDINH/MIL, 34,910-pyrenetetracarboxydiimine (Materials of Institute Lavoisier).

Results and discussion

Dose influence on the degradation of CQ

The stepwise absorption reduction observed for CQ solution at 343 nm and at 330 nm with increasing radiation dose from 0 kGy to 7 kGy is illustrated in Fig. 1. Additionally, the corresponding reduction in CQ concentrations with increasing dose is shown in Fig. 2. The concentration of CQ was reduced from 125 mg·L⁻¹ to 22 mg·L⁻¹, which corresponds to an 82% reduction in the initial CQ concentration following electron beam irradiation. At the lowest absorbed dose achieved in this experiment (0.5 kGy), the initial CQ concentration of 125 mg·L⁻¹ was reduced by ≈50%.

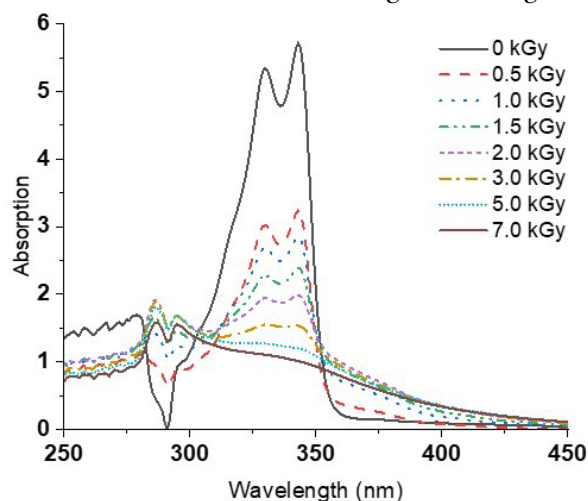Free radicals generated during the radiolysis of water drive the reactions leading to the degradation of organic compounds in water. These radicals are generated through a combination of physical, physical-chemical, and chemical processes that occur within 10^{-12} s following the interactions of radiation in the water matrix. The species formed and their corresponding G-values are presented in Table 2.

The hydroxyl radical and hydrated electron play important roles in the degradation of CQ molecules via the addition reaction and dissociative electron attachment according to Eqs. (1) and (2), respectively. Reaction rates for the reactions with $^{\bullet}OH$ and e_{aq}^{-} at a pH of 8.5 have been previously evaluated and are shown in Table 2 [47].

$$(1) \quad {}^{\bullet}OH + C_{18}H_{26}N_3Cl \rightarrow C_{18}H_{26}N_3ClOH$$

$$(2) \quad e_{aq}^{-} + C_{18}H_{26}N_3Cl \rightarrow C_{18}H_{26}N_3^{\bullet} + Cl^{-}$$

Fig. 1. UV-VIS absorption spectrum for 125 mg·L⁻¹ chloroquine solution observed at 343 nm at irradiation doses ranging from 0 kGy to 7 kGy.
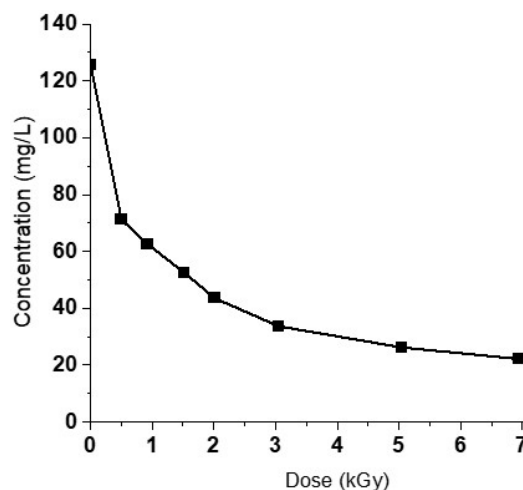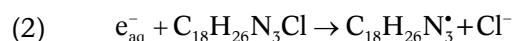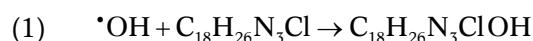

Fig. 2. Degradation of 125 mg·L⁻¹ of chloroquine solution under EB radiation.

Table 2. Species formed in the radiolysis of water and their corresponding G-values and reaction rates (k) with CQ

Species	G $(mmol \cdot J^{-1})$	Molecules/100 eV	k $(dm^3 \cdot mol^{-1} \cdot s^{-1})$
e_{aq}^-	0.28	2.8	4.8×10^{10}
$^{\bullet}OH$	0.28	2.8	7.3×10^9
$^{\bullet}H$	0.06	0.6	–
H_3O^+	0.26	2.6	–
H_2	0.045	0.45	
H_2O_2	0.07	0.7	

Effects of CQ concentration

Initial concentrations of CQ were varied to study the effect of CQ concentration on the degradation efficiency. The removal efficiency decreased with increasing CQ concentration at the same applied radiation dose (Fig. 3a). Generally, concentrations of CQ between 25 mg·L^{-1} and 125 mg·L^{-1} have degradation efficiencies ≥75% for a maximum radiation dose of 7 kGy. However, for lower concentrations (25 mg·L^{-1}), more than 99% removal efficiency was achieved.

The degradation of CQ can be represented using a pseudo-first-order relation (Eq. (3)) [48].

$$(3) \qquad -\ln \frac{[C]}{[C_0]} = kD$$

where C and C_0 are the final and initial concentrations of the target compound at a dose D (kGy) with a rate constant of k. The results of the k values at different concentrations at 0.5 kGy are shown in Fig. 3b. The reaction rate is observed to decrease with increasing concentrations of CQ in the water as shown in Fig. 3c and Table 3.

Initial solution pH

The solvent pH influences the percentage of the different radicals generated during the radiolysis of the water. Under alkaline conditions, $^{\bullet}OH$ readily reacts with OH^- to generate $O^{\bullet-}$ thereby reducing the concentration of $^{\bullet}OH$ and hence the degradation efficiency.

$$(4) \qquad ^{\bullet}OH + OH^- \rightarrow O^{\bullet-} + H_2O$$
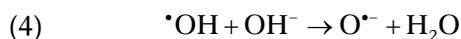
In acidic media, the hydrated electrons e_{aq}^- react with H^+ to produce $^{\bullet}H$.

$$(5) \qquad e_{aq}^- + H^+ \rightarrow {}^{\bullet}H$$

Therefore, under electron beam irradiation, the pH enhances or inhibits the production of reactive oxidizing or reducing species and therefore affects the degradation process. In this study, the degradation of CQ was observed to increase with increasing pH. The removal efficiency decreased slightly with increasing pH at irradiation doses between 0.5 kGy and 2 kGy. The acidic pH of 2 to neutral pH of 7 had relatively higher removal efficiencies for CQ (≈84%). In neutral to an alkaline pH of 10, the removal ef-
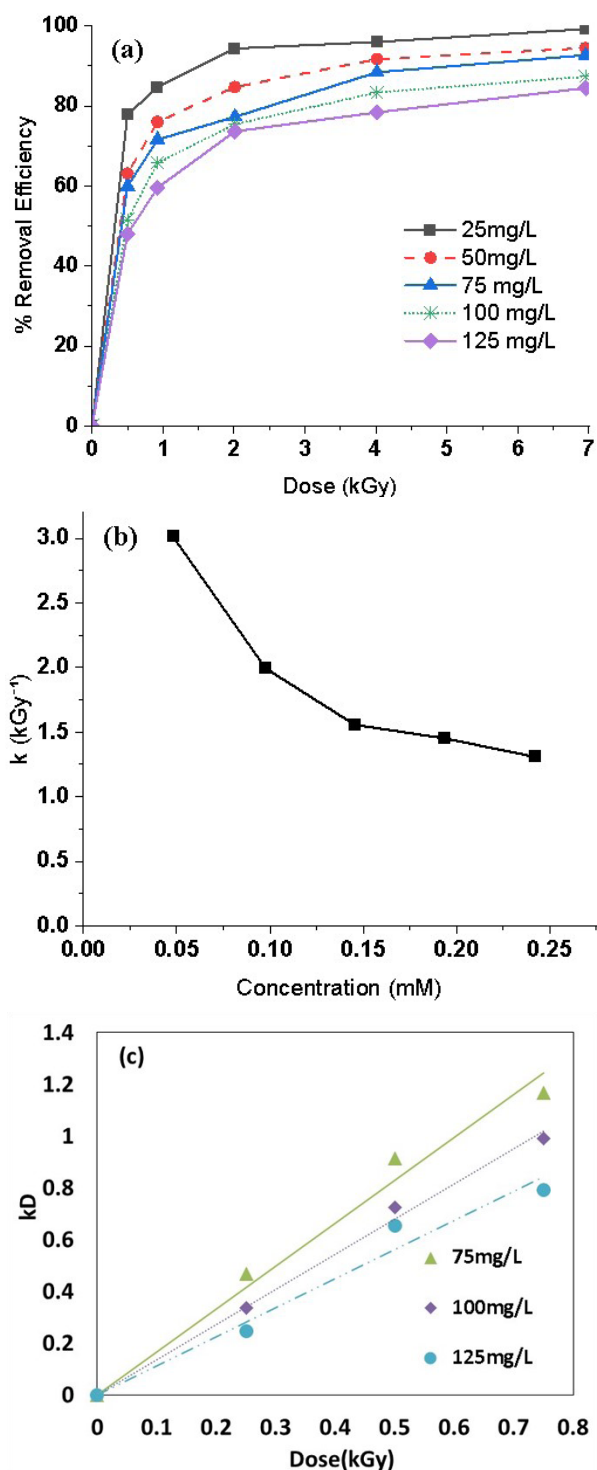
Fig. 3. Degradation of different concentrations of chloroquine solutions under EB irradiation. (a) Removal efficiency of chloroquine at different initial concentrations. (b) k (kGy^{-1}) values for removal of chloroquine at 0.5 kGy. (c) Plot of the rate constant against dose.

Table 3. Reaction rates (k) for degradation of different concentrations of chloroquine and corresponding R^2

Concentration CQ (mg·L^{-1})	k (kGy^{-1})	R^2
75	1.6567	0.9935
100	1.3603	0.9982
125	1.1224	0.9891

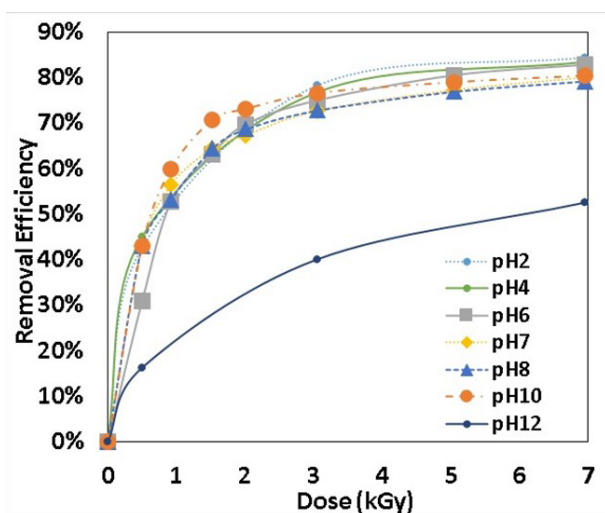**Fig. 4.** Removal efficiency of 125 mg·L⁻¹ of chloroquine solution under EB irradiation at different initial pH.

ficiency was at ≈80% at irradiation doses of 7 kGy (Fig. 4). However, slight increments in the removal efficiency were observed with increasing pH from neutral to pH = 10 at an irradiation dose of 3 kGy. According to Eq. (2), reactions with the hydrated electron have a higher reaction rate compared to hydroxyl radical reactions. More hydrated electrons are produced in alkaline conditions, which lead to higher degradation of CQ. However, in strongly alkaline conditions (pH = 12), the removal efficiency was inhibited. This could be attributed to the reactions of hydroxyl radicals with hydroxide (Eq. (4)). Conversely, at lower pH, hydrated electrons are consumed, which would result in lower removal efficiency for CQ. Additionally, hydroxyl radicals are known to have a higher reduction potential (2.72 V) at acidic pH compared to alkaline conditions (1.89 V); therefore, their role in CQ degradation would be affected at different pH [49].

The changes in the initial pH during the irradiation process are presented in Fig. 5. Other than affecting the production of water radiolysis products, the pH value can affect the reaction pathways by changing the structure and characteristics of
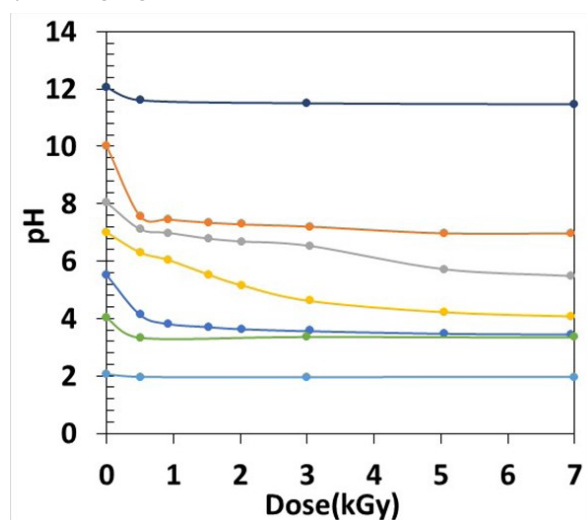
contaminants such as their solubility. Certain compounds retain their molecular form when the pH is less than its pK_a. However, when the pH $>pK_a$, the compound loses a proton and becomes negatively charged. The pKa of CQ is 8.76, and it is a weak acid with a tendency to donate electrons. Therefore, at pH $<pKa$ (between pH 2 and 7), CQ is in the non--ionic form (protonated). At pH >7, the divalent form of CQ (CQH_2^{2+}) is dominant alongside lesser concentrations of the monovalent and neutral CQ [50]. Compounds such as diclofenac are insoluble at low pH values (around 3), which is a favorable condition for electron beam irradiation. Therefore, the optimization of pH may influence the solubility and degradation of some pollutants [51]. Neutral or acidic media are preferable to an alkaline solution for the degradation of HCQ, a CQ derivative under gamma irradiation [52, 53]. In the present study, acidic to neutral pH favors the degradation of CQ under an electron beam. Acidic pH has been reported to favor electro-Fenton oxidation, sulfate radical AOPs, and the Fe(VI) oxidation of CQ (Table 1). The pH of wastewater is a vital component before and after treatment for the eventual discharge of wastewater.

Degradation byproducts

The results for the degradation byproducts are based on the degradation of 125 mg·L⁻¹ of CQ solution under electron beam irradiation. The CQ solution was irradiated between 0.5 kGy and 7 kGy. The presence and degradation of organic compounds influence parameters used in wastewater such as pH, TOC, COD, chloride ion, and nitrogen. The formation or reduction in these physicochemical parameters was used to evaluate the effectiveness of CQ treatment under electron beam irradiation.

Change in the solution pH

During the radiolysis of the CQ solutions, the pH was observed to reduce from 6.5 before irradiation to 3.2 at 7 kGy (Fig. 6). A similar decrease in pH has been observed in the degradation of ciprofloxacin
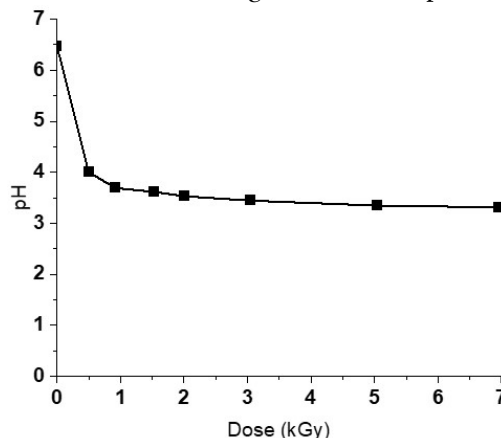

Fig. 5. Changes in the pH of the solution with dose during the degradation of 125 mg·L⁻¹ chloroquine solution.

Fig. 6. Changes in the pH concentration during EB irradiation of 125 mg·L⁻¹ chloroquine. The pH varied from slightly acidic before irradiation to acidic at the end of irradiation.

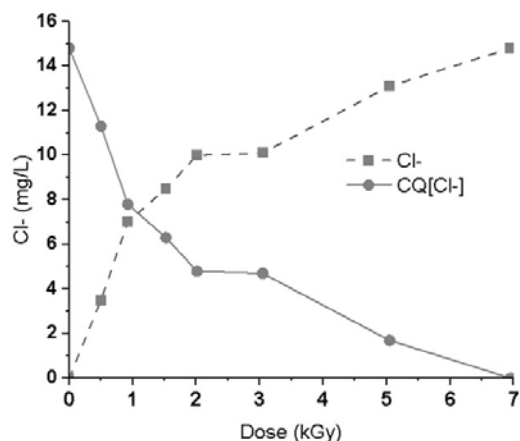**Fig. 7.** Release of Cl⁻ with increasing dose during radiolysis of chloroquine (125 mg·L⁻¹) solution under the EB treatment.

where pH decreased from 7.00 to 4.22 at 5.0 kGy, consistent with the formation of lower molecular weight organic acids and dissolved ions resulting from EB treatment [51, 54].

In the degradation of CQ under electro-Fenton oxidation, the change in pH was attributed to the formation of carboxylic acids such as oxamic and oxalic acids [20]. Additionally, pH changes in the degradation of diuron under radiation were attributed to the formation of aldehydes and ketones [55].

Cl⁻ generation

During the radiolysis of organic compounds with good leaving groups such as halogenated compounds, dissociative electron attachment as shown in Eq. (2) is proposed to be the most preferred reaction process of the aqueous electron [56, 57]. The Cl⁻ ions present in CQ were continuously released with increasing radiation dose (Fig. 7). Almost complete Cl⁻ detachment was observed at 7 kGy indicative of the dechlorination of the CQ compound.

Most polychlorinated cyclic compounds are stable, lipophilic, and tend to bioaccumulate in the environment with slow degradation. Chlorinated compounds i.e., pesticides, biphenyls, dibenzodioxins, and dibenzofurans are genotoxic (mutagenic and carcinogenic) and therefore pose a risk to living organisms [58–60]. Therefore, the dechlorination of CQ under electron beam treatment would be considered to reduce its toxicity. However, in the present study, no toxicity studies were undertaken to ascertain the reduction in toxicity.

Nitrogen

The generation of NO_3^- and NO_2^- in the aqueous phase in the presence of ionizing radiation is normal when dealing with nitrogen-containing compounds [49]. The oxidative degradation of nitrogen-containing compounds releases nitrate, nitrite, and ammonium ions [61, 62]. Nitrogen often enters water and wastewater via agricultural, domestic, and manufacturing wastes. The ammonium, organic nitrogen, nitrate, and nitrite concentrations are the
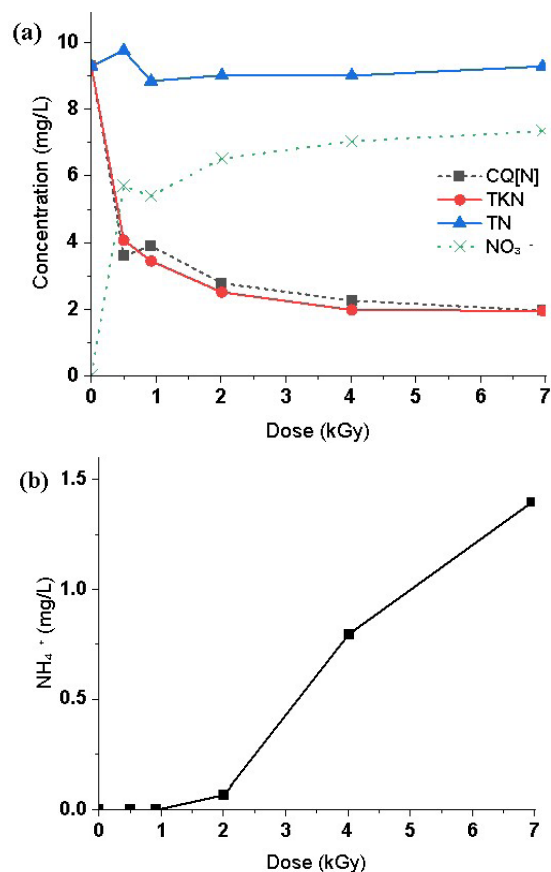

Fig. 8. (a) Reduction in total Kjeldahl nitrogen, formation of NO_3^-, and (b) generation of NH_4^+ in the degradation of 125 mg·L⁻¹ of chloroquine solution under EB irradiation.

most relevant for the determination of nitrogen in water and wastewater. The total organic bound nitrogen (CQ[N]) was reduced by 50% as well as the TKN (Fig. 8). The eventual formation of inorganic nitrogen (NO_3^-) is also observed to increase with increasing doses. Additionally, the formation of the NH_4^+ ions with increasing dose was observed alluding to the nitrification process.

Organic nitrogen (TKN) is normally converted into inorganic nitrogen (NO_3^- and NO_2^-) during the wastewater-treatment processes. At the end of the water-treatment process, predominantly inorganic nitrogen is present. Nitrogen in freshly polluted water is originally present in the form of organic nitrogen and ammonia (TKN + NH_3). Completely nitrified wastewater will have little or no organic nitrogen. However, secondary reactions of mineralized nitrogen species (nitrate and nitrite ions) with the parent or intermediate compound generate nitrogenous disinfection byproducts that are also a concern [61].

Changes in the oxygen demand

Dissolved oxygen (DO) reflects the amount of oxygen dissolved in water and is available to living aquatic organisms. The decay of organic matter consumes the DO and the presence of excess organic material, biochemical oxygen demand (BOD), or COD in lakes and rivers causes eutrophication (oxygen deficiency). A large amount of
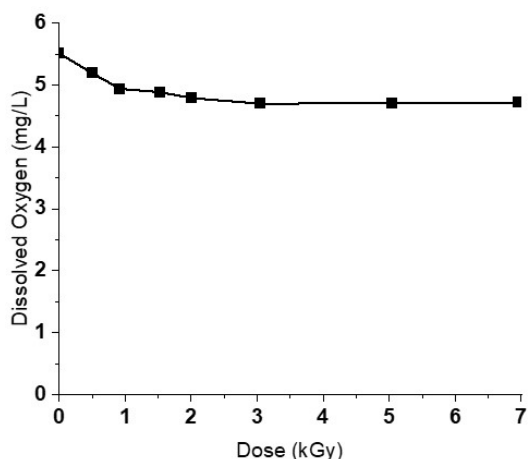
Fig. 9. Changes in dissolved oxygen concentration during electron beam irradiation of 125 mg·L^{-1} chloroquine solution.

DO is consumed by aerobic microorganisms to decompose the organic matter. The DO is affected by the water temperature, salt concentration, atmospheric pressure, and other conditions, and the saturation level decreases with increases in water temperature. During the radiolysis processing of wastewater, the DO will react with radicals formed. This may significantly reduce O_2 concentrations. However, from the experiment, the dissolved O_2 varied from 5.5 mg·L^{-1} before irradiation to 4.7 mg·L^{-1} at 7 kGy as shown in Fig. 9.

High DO has been found to influence the mineralization of azo dyes under electron beam irradiation by improving the cleavage of the aromatic rings and promoting the reduction of TOC [63]. The DO was more important for the destruction of substituted aromatic rings in the dye molecule than the chromophore and needed to be maintained at optimal concentrations during electron beam radiolysis [64]. However, DO scavenges e_{aq}^- and H$^{\bullet}$, therefore, reducing the equilibrium concentration of these species and their reactions with target pollutants [65].

The oxygen demand determines the amount of organic pollution in water, waste loadings of treatment plants, and in evaluating the efficiency of treatment processes. BOD, COD, and TOC are used to measure the oxygen demand. There was a slight
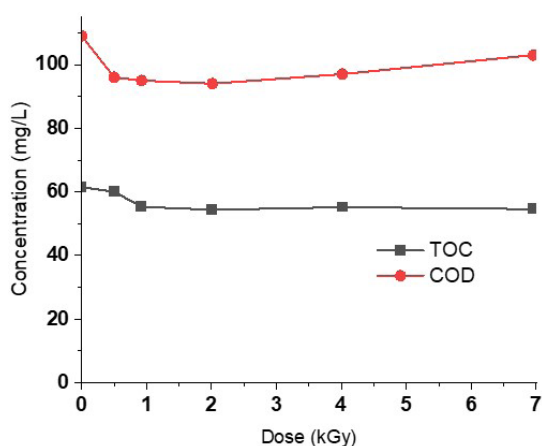

Fig. 10. Variation in COD and TOC during EB degradation of 125 mg·L^{-1} solution of chloroquine.

decrease in the COD and TOC with increasing doses and the decreasing concentration of CQ (Fig. 10). These observations in TOC and COD degradation indicate the formation of other organic byproducts that are not easily degraded in the present conditions [66]. In other studies, even with the apparent insignificant reduction in COD and TOC, the resulting degradation products exhibited a higher biological oxygen demand and therefore were more susceptible to biological degradation.

Conclusions

CQ solution of 125 mg·L^{-1} concentration has been degraded with an efficiency of 82% under an electron beam process at doses ranging from 0.5 kGy to 7 kGy in ambient conditions. Both the hydroxyl radical and hydrated electron played roles in the decomposition of CQ molecules. The initial concentration of the CQ solution affected the degradation and the reaction rate; hence, the degradation efficiencies decreased with increasing CQ concentrations under electron beam treatment. The release of chloride ions was considered indicative of the dissociative electron-attachment process during the electron beam processing of the CQ solution. Dechlorination could imply a reduction in the toxicity of the resulting products. The pH of 125 mg·L^{-1} of the CQ solution was measured and observed to drop from the initial pH of 6 to a pH of 3.5 at the end of processing. This can be attributed to the formation of lower molecular weight carboxylic acids and ions as has been reported in other studies. It was observed that at acidic pH, the removal efficiency was higher than at neutral pH. However, alkaline pH exhibited increased removal efficiency. This could be attributed to the state of the CQ molecule at different pH (protonation). Additionally, the effects of pH during the radiolysis of water affect the radiolysis products ($^{\bullet}$OH and e_{aq}^-), which play the main roles in the degradation of CQ. However, in strongly alkaline conditions, degradation was inhibited. The degradation of 125 mg·L^{-1} of CQ did not lead to complete mineralization evident from the insignificant COD and TOC reduction. This indicates the formation of organic compounds less susceptible to degradation by the electron beam process. However, from this study, it can be concluded that EB processing can degrade 125 mg·L^{-1} of CQ solution. Additionally, at lower pollutant concentrations, the removal efficiency is higher.

ORCID

S. Bułka http://orcid.org/0000-0002-0377-1535
A. G. Chmielewski http://orcid.org/0000-0001-6262-5952
S. Kabasa http://orcid.org/0000-0002-0039-9205
Y. Sun http://orcid.org/0000-0002-7359-3869

References

1. Abena, P. M., Decloedt, E. H., Bottieau, E., Suleman, F., Adejumo, P., Sam-Agudu, N. A., Muyembe TamFum, J. J., Seydi, M., Eholie, S. P., Mills, E. J., Kallay, O., Zumla, A., & Nachega, J. B. (2020). Chloroquine and hydroxychloroquine for the prevention or treatment of COVID-19 in Africa: Caution for inappropriate off-label use in healthcare settings. *Am. J. Trop. Med. Hyg.*, *102*(6). https://doi.org/10.4269/ajtmh.20-0290.

2. Nippes, R. P., Macruz, P. D., da Silva, G. N., & Neves Olsen Scaliante, M. H. (2021). A critical review on environmental presence of pharmaceutical drugs tested for the COVID-19 treatment. *Process Saf. Environ. Protect.*, *152*. https://doi.org/10.1016/j.psep.2021.06.040.

3. Gwenzi, W., Selvasembian, R., Offiong, N. A. O., Mahmoud, A. E. D., Sanganyado, E., & Mal, J. (2022). COVID-19 drugs in aquatic systems: a review. *Environ. Chem. Lett.*, *20*(2). https://doi.org/10.1007/s10311-021-01356-y.

4. Yakubu, O. H. (2017). Pharmaceutical wastewater effluent-source of contaminants of emerging concern: Phytotoxicity of metronidazole to soybean (Glycine max). *Toxics*, *5*(2). https://doi.org/10.3390/toxics5020010.

5. Carter, L. J., Chefetz, B., Abdeen, Z., & Boxall, A. B. A. (2019). Emerging investigator series: Towards a framework for establishing the impacts of pharmaceuticals in wastewater irrigation systems on agro-ecosystems and human health. *Environ. Sci.-Processes and Impacts*, *21*(4). https://doi.org/10.1039/c9em00020h

6. Jjemba, P. K. (2002). The effect of chloroquine, quinacrine, and metronidazole on both soybean plants and soil microbiota. *Chemosphere*, *46*(7), 1019–1025. https://doi.org/10.1016/S0045-6535(01)00139-4

7. Jjemba, P. K. (2002). The potential impact of veterinary and human therapeutic agents in manure and biosolids on plants grown on arable land: A review. *Agriculture, Ecosystems and Environment*, *93*(1/3), 267–278. https://doi.org/10.1016/S0167-8809(01)00350-4.

8. Tanoue, R., Sato, Y., Motoyama, M., Nakagawa, S., Shinohara, R., & Nomiyama, K. (2012). Plant uptake of pharmaceutical chemicals detected in recycled organic manure and reclaimed wastewater. *J. Agric. Food Chem.*, *60*(41). https://doi.org/10.1021/jf303142t.

9. Doddaga, S., & Peddakonda, R. (2013). Chloroquine-N-oxide, a major oxidative degradation product of chloroquine: Identification, synthesis and characterization. *J. Pharm. Biomed. Anal.*, *81/82*, 118–125. https://doi.org/10.1016/J.JPBA.2013.04.004.

10. Kuroda, K., Li, C., Dhangar, K., & Kumar, M. (2021). Predicted occurrence, ecotoxicological risk and environmentally acquired resistance of antiviral drugs associated with COVID-19 in environmental waters. *Sci. Total Environ.*, *776*, 145740. https://doi.org/10.1016/J.SCITOTENV.2021.145740.

11. Liu, Y., Zou, D., & Gao, Y. (2022). Performance of high temperature phase-stable high entropy oxide (MgCuMnCoFe)Ox in catalytic wet air oxidation of chloroquine phosphate. *J. Mat. Sci.*, *57*, 9104–9117. https://doi.org/10.1007/s10853-022-07271-z.

12. Revilla Pacheco, C., Terán Hilares, R., Colina Andrade, G., Mogrovejo-Valdivia, A., & Pacheco Tanaka, D. A. (2021). Emerging contaminants, SARS-COV-2 and wastewater treatment plants, new challenges to confront: A short review. *Bioresource Technology Reports*, *15*, 100731. https://doi.org/10.1016/J.BITEB.2021.100731.

13. Ganguly, A., & Hwa, K. Y. (2022). Construction of zinc selenide microspheres decorated with octadecylamine-functionalized reduced graphene oxide as an effective catalyst for the dual-mode detection of chloroquine phosphate. *Mater. Today Chem.*, *24*, 100862. https://doi.org/10.1016/J.MTCHEM.2022.100862.

14. He, Y., Sun, J., Yao, W., Lu, K., Liu, D., Xie, H., Huang, C., & Jia, N. (2023). A self-powered photoelectrochemical molecular imprinted sensor for chloroquine phosphate with enhanced cathodic photocurrent via stepped energy band alignment engineering. *Chem. Eng. J.*, *451*, 138748. https://doi.org/10.1016/J.CEJ.2022.138748.

15. Hayden, K. R., Preisendanz, H. E., Jones, M., Elkin, K. E., Shreve, M. J., Clees II, W. I., Clark, S., Mashtare, M. L., Veith, T. L., Elliott, H. A., Watson, J. E., Silverman, J., Richard, T. L., & Read, A. R. (2022). Impacts of the COVID-19 pandemic on pharmaceuticals in wastewater treated for beneficial reuse: Two case studies in central Pennsylvania. *J. Environ. Qual.*, *51*, 1066–1082.

16. Saim, S., & Behira, B. (2021). Impact of chloroquine as treatment of pandemic COVID-19 on environment. *J. Mat. Environ. Sci.*, *13*(4), 1017–1024.

17. Morales-Paredes, C. A., Rodríguez-Díaz, J. M., & Boluda-Botella, N. (2022). Pharmaceutical compounds used in the COVID-19 pandemic: A review of their presence in water and treatment techniques for their elimination. *Sci. Total Environ.*, *814*, 152691. https://doi.org/10.1016/J.SCITOTENV.2021.152691.

18. Yi, X. H., Ji, H., Wang, C. C., Li, Y., Li, Y. H., Zhao, C., Wang, A., Fu, H., Wang, P., Zhao, X., & Liu, W. (2021). Photocatalysis-activated SR-AOP over PDINH/MIL-88A(Fe) composites for boosted chloroquine phosphate degradation: Performance, mechanism, pathway and DFT calculations. *Appl. Catal. B-Environ.*, *293*, 120229. https://doi.org/10.1016/J.APCATB.2021.120229.

19. Dong, F., Li, J., Lin, Q., Wang, D., Li, C., Shen, Y., Zeng, T., & Song, S. (2022). Oxidation of chloroquine drug by ferrate: Kinetics, reaction mechanism and antibacterial activity. *Chem. Eng. J.*, *428*. https://doi.org/10.1016/j.cej.2021.131408.

20. Midassi, S., Bedoui, A., & Bensalah, N. (2020). Efficient degradation of chloroquine drug by electro-Fenton oxidation: Effects of operating conditions and degradation mechanism. *Chemosphere*, *260*, 127558. https://doi.org/10.1016/j.chemosphere.2020.127558.

21. Cornejo, O. M., Murrieta, M. F., Castañeda, L. F., & Nava, J. L. (2021). Electrochemical reactors equipped with BDD electrodes: Geometrical aspects and ap-

plications in water treatment. *Curr. Opin. Solid State Mat. Sci.*, *25*(4), 100935. https://doi.org/10.1016/J.COSSMS.2021.100935.

22. Quang, H. H. P., Dinh, N. T., Thi, T. N. T., Bao, L. T. N., Yuvakkumar, R., & Nguyen, V. H. (2022). Fe2+, Fe3+, Co2+ as highly efficient cocatalysts in the homogeneous electro-Fenton process for enhanced treatment of real pharmaceutical wastewater. *J. Water Process. Eng.*, *46*, 102635. https://doi.org/10.1016/J.JWPE.2022.102635.

23. Yang, J., Zhu, M., & Dionysiou, D. D. (2021). What is the role of light in persulfate-based advanced oxidation for water treatment? *Water Res.*, *189*, 116627. https://doi.org/10.1016/J.WATRES.2020.116627.

24. Peng, X., Wu, J., Zhao, Z., Wang, X., Dai, H., Wei, Y., Xu, G., & Hu, F. (2022). Activation of peroxymonosulfate by single atom Co-N-C catalysts for high-efficient removal of chloroquine phosphate via non-radical pathways: Electron-transfer mechanism. *Chem. Eng. J.*, *429*, 132245. https://doi.org/10.1016/J.CEJ.2021.132245.

25. Dan, J., Rao, P., Wang, Q., Zhang, M., He, Z., Zhang, W., Gao, N., Deng, J., & Chen, J. (2022). Catalytic performance of wrapped CoO by MgO in oxidative degradation of chloroquine phosphate with peroxymonosulfate. *Appl. Surf. Sci.*, *573*, 151430. https://doi.org/10.1016/J.APSUSC.2021.151430.

26. Guo, Z., Zhang, Y., Gan, S., He, H., Cai, N., Xu, J., Guo, P., Chen, B., & Pan, X. (2022). Effective degradation of COVID-19 related drugs by biochar-supported red mud catalyst activated persulfate process: Mechanism and pathway. *J. Clean Prod.*, *340*, 130753. https://doi.org/10.1016/J.JCLEPRO.2022.130753.

27. Atunwa, B. T., Dada, A. O., Inyinbor, A. A., & Pal, U. (2022). Synthesis, physiochemical and spectroscopic characterization of palm kernel shell activated carbon doped AgNPs (PKSAC@AgNPs) for adsorption of chloroquine pharmaceutical waste. *Mater. Today-Proceedings*, *65*, 3538–3546. https://doi.org/10.1016/J.MATPR.2022.06.099.

28. Dada, A. O., Inyinbor, A. A., Bello, O. S., & Tokula, B. E. (2021). Novel plantain peel activated carbon–supported zinc oxide nanocomposites (PPAC-ZnO-NC) for adsorption of chloroquine synthetic pharmaceutical used for COVID-19 treatment. *Biomass Convers. Biorefinery*, *13*, 9181–9193. https://doi.org/10.1007/s13399-021-01828-9.

29. Bezerra de Araujo, C. M., Wernke, G., Ghislandi, M. G., Diório, A., Vieira, M. F., Bergamasco, R., Alves da Motta Sobrinho, M., & Rodrigues, A. E. (2023). Continuous removal of pharmaceutical drug chloroquine and Safranin-O dye from water using agar-graphene oxide hydrogel: Selective adsorption in batch and fixed-bed experiments. *Environ. Res.*, *216*, 114425. https://doi.org/10.1016/J.ENVRES.2022.114425.

30. Januário, E. F. D., Fachina, Y. J., Wernke, G., Demiti, G. M. M., Beltran, L. B., Bergamasco, R., & Vieira, A. M. S. (2022). Application of activated carbon functionalized with graphene oxide for efficient removal of COVID-19 treatment-related pharmaceuticals from water. *Chemosphere*, *289*, 133213. https://doi.org/10.1016/J.CHEMOSPHERE.2021.133213.

31. Mojiri, A., Zhou, J. L., Nazari, V. M., Rezania, S., Farraji, H., & Vakili, M. (2022). Biochar enhanced the performance of microalgae/bacteria consortium for insecticides removal from synthetic wastewater. *Process Saf. Environ. Protect.*, *157*, 284–296. https://doi.org/10.1016/J.PSEP.2021.11.012.

32. Nkwoada, A. U., Alisa, C. D., Oguwike, M. M., & Amaechi, I. A. (2022). Removal of aspirin and chloroquine from aqueous solution using organo-clay derived from kaolinite. *Journal of Physics and Chemistry of Materials*, *9*(1), 1–11. https://www.isroset.org/journal/JPCM/archive_issue.php?pub_id=359.

33. Lindroos, M., Hörnström, D., Larsson, G., Gustavsson, M., & van Maris, A. J. A. (2019). Continuous removal of the model pharmaceutical chloroquine from water using melanin-covered *Escherichia coli* in a membrane bioreactor. *J. Hazard. Mater.*, *365*, 74–80. https://doi.org/10.1016/j.jhazmat.2018.10.081.

34. Vidovix, T. B., Januário, E. F. D., Bergamasco, R., & Vieira, A. M. S. (2022). Evaluation of agro-industrial residue functionalized with iron oxide magnetic nanoparticles for chloroquine removal from contaminated water. *Mater. Lett.*, *326*, 132915. https://doi.org/10.1016/J.MATLET.2022.132915.

35. Sun, H., He, J., Liu, Y., Ji, X., Wang, G., Yang, X., & Zhang, Y. (2023). Removal performance and mechanism of emerging pollutant chloroquine phosphate from water by iron and magnesium Co-modified rape straw biochar. *Molecules*, *28*(8), 3290. https://doi.org/10.3390/MOLECULES28083290.

36. Wang, F. X., Wang, C. C., Du, X., Li, Y., Wang, F., & Wang, P. (2022). Efficient removal of emerging organic contaminants via photo-Fenton process over micronsized Fe-MOF sheet. *Chem. Eng. J.*, *429*, 132495. https://doi.org/10.1016/J.CEJ.2021.132495.

37. Hu, Z., Luo, J., Xu, S., Yuan, P., Guo, S., Tang, X., & Shen, B. (2023). Activation of peroxymonosulfate using spent Li-ion batteries for the efficient degradation of chloroquine phosphate. *Catalysts*, *13*(4), 661. https://doi.org/10.3390/CATAL13040661.

38. Li, Y., Xu, B. H., Deng, L., & Luo, W. (2022). Degradation of chloroquine phosphate by UV-activated persulfate. *Huanjing Kexue/Environmental Science*, *43*(9). https://doi.org/10.13227/j.hjkx.202110030.

39. Elkacmi, R., Zahnoune, R., El Amri, R., & Boudouch, O. (2023). Application of electrocoagulation process for the removal of chloroquine from an aqueous solution. *H2Open J.* https://doi.org/10.2166/h2oj.2023.016.

40. Regalado-Méndez, A., Zavaleta-Avendaño, J., Peralta-Reyes, E., & Natividad, R. (2023). Convex optimization for maximizing the degradation efficiency of chloroquine in a flow-by electrochemical reactor. *J. Solid State Electrochem.*, *27*, 3163–3176. https://doi.org/10.1007/s10008-023-05452-7.

41. Lin, Y., Chen, Y., Chen, J., Chen, J., Yang, L., Wei, W., Ni, B. J., & Chen, X. (2023). Efficient chloroquine removal by electro-Fenton with FeS2-modified cathode: Performance, influencing factors, pathway contributions, and degradation mechanisms. *ACS EST Water*, *3*(8), 2786–2796. https://doi.org/10.1021/acsestwater.3c00283.

42. Gustavsson, M., Hörnström, D., Lundh, S., Belotserkovsky, J., & Larsson, G. (2016). Biocatalysis on the surface of *Escherichia coli*: Melanin pigmentation of the cell exterior. *Sci. Rep.*, *6*. https://doi.org/10.1038/srep36117.

43. Han, B., Ko, J., Kim, J., Kim, Y., Chung, W., Makarov, I. E., Ponomarev, A. V., & Pikaev, A. K. (2002). Combined electron-beam and biological treatment of dyeing complex wastewater. Pilot plant experiments. *Radiat. Phys. Chem.*, *64*(1), 53–59. https://doi.org/10.1016/S0969-806X(01)00452-2.

44. Sharpe, P. H. G., & Sehested, K. (1989). The dichromate dosimeter: A pulse-radiolysis study. *Int. J. Radiat. Appl. Instrum. C-Radiat. Phys. Chem.*, *34*(5), 763–768. https://doi.org/10.1016/1359-0197(89)90281-6.

45. McLaughlin, W. L., Al-Sheikhly, M., Farahani, M., & Hussmann, M. H. (1990). A sensitive dichromate dosimeter for the dose range, 0.2-3 kGy. *Int. J. Radiat. Appl. Instrum. C-Radiat. Phys. Chem.*, *35*(4/6), 716–723. https://doi.org/10.1016/1359-0197(90)90303-Y.

46. Šećerov, B., & Bačić, G. (2008). Comparison of dichromate and ethanol-chlorobenzene dosimeters in high dose radiation processing. *Nukleonika*, *53*(3), 85–87.

47. Bors, W., Golenser, J., Chevion, M., & Saran, M. (1991). Reductive and oxidative radical reactions of selected antimalarial drugs. *Oxidative Damage & Repair*, *1991*, 234–240. https://doi.org/10.1016/B978-0-08-041749-3.50046-2.

48. Chen, X., & Wang, J. (2021). Degradation of antibiotic cephalosporin C in different water matrices by ionizing radiation: Degradation kinetics, pathways, and toxicity. *Sci. Total Environ.*, *791*, 148253. https://doi.org/10.1016/J.SCITOTENV.2021.148253.

49. Dey, G. R. (2011). Nitrogen compounds' formation in aqueous solutions under high ionizing radiation: An overview. *Radiat. Phys. Chem.*, *80*(3), 394–402. https://doi.org/10.1016/J.RADPHYSCHEM.2010.10.010.

50. Klouda, C. B., & Stone, W. L. (2020). Oxidative stress, proton fluxes, and chloroquine/hydroxychloroquine treatment for COVID-19. *Antioxidants*, *9*(9). https://doi.org/10.3390/antiox9090894.

51. Mirzaei, A., Chen, Z., Haghighat, F., & Yerushalmi, L. (2017). Removal of pharmaceuticals from water by homo/heterogonous Fenton-type processes – A review. *Chemosphere*, *174*, 665–688. https://doi.org/10.1016/J.CHEMOSPHERE.2017.02.019.

52. Boujelbane, F., Nasr, K., Sadaoui, H., Bui, H. M., Gantri, F., & Mzoughi, N. (2022). Decomposition mechanism of hydroxychloroquine in aqueous solution by gamma irradiation. *Chem. Pap.*, *76*(3), 1777–1787. https://link.springer.com/article/10.1007/s11696-021-01969-1.

53. Zaouak, A., Jebali, S., Chouchane, H., & Jelassi, H. (2023). Impact of gamma-irradiation on the degradation and mineralization of hydroxychloroquine aqueous solutions. *Int. J. Environ. Sci. Technol.*, *20*, 6815–6824. https://doi.org/10.1007/s13762-022-04360-z.

54. Kiyoshi Tominaga, F., Fonseca Boiani, N., Tieko Silva, T., Gomes dos Santos, J., Temponi Lebre, D., Leo, P., & Borrely, I. S. (2023). Electron beam irradiation applied for the detoxification and degradation of single ciprofloxacin aqueous solution and multiclass pharmaceutical quaternary mixture. *Sep. Purif. Technol.*, *307*, 122818. https://doi.org/10.1016/J.SEPPUR.2022.122818.

55. Kovács, K., He, S., Mile, V., Csay, T., Takács, E., & Wojnárovits, L. (2015). Ionizing radiation induced degradation of diuron in dilute aqueous solution. *Chem. Cent. J.*, *9*(1), 1–10. https://doi.org/10.1186/s13065-015-0097-0.

56. McAllister, M., Kazemigazestane, N., Henry, L. T., Gu, B., Fabrikant, I., Tribello, G. A., & Kohanoff, J. (2019). Solvation effects on dissociative electron attachment to thymine. *J. Phys. Chem. B*, *123*(7). https://doi.org/10.1021/acs.jpcb.8b11621.

57. Wang, F., Archirel, P., Muroya, Y., Yamashita, S., Pernot, P., Yin, C., El Omar, A. K., Schmidhammer, U., Teuler, J. M., & Mostafavi, M. (2017). Effect of the solvation state of electron in dissociative electron attachment reaction in aqueous solutions. *Phys. Chem. Chem. Phys.*, *19*(34), 23068–23077. https://doi.org/10.1039/C7CP03997B.

58. Jayaraj, R., Megha, P., & Sreedev, P. (2016). Organochlorine pesticides, their toxic effects on living organisms and their fate in the environment. *Interdiscipl. Toxicol.*, *9*(3/4), 90–100. https://doi.org/10.1515/intox-2016-0012.

59. Adeola, A. O. (2018). Fate and toxicity of chlorinated phenols of environmental implications: A review. *Medicinal & Analytical Chemistry International Journal*, *2*(4), 1–8. https://doi.org/10.23880/macij-16000126.

60. Henschler, D. (1994). Toxicity of chlorinated organic compounds: Effects of the introduction of chlorine in organic molecules. *Angewandte Chemie International*, *33*(19), 1920–1935. https://doi.org/10.1002/ANIE.199419201.

61. Rayaroth, M. P., Aravindakumar, C. T., Shah, N. S., & Boczkaj, G. (2022). Advanced oxidation processes (AOPs) based wastewater treatment – unexpected nitration side reactions – a serious environmental issue: A review. *Chem. Eng. J.*, *430*, 133002. https://doi.org/10.1016/J.CEJ.2021.133002.

62. Maletzky, P., & Bauer, R. (1998). The photo-Fenton method – degradation of nitrogen containing organic compounds. *Chemosphere*, *37*(5), 899–909. https://doi.org/10.1016/S0045-6535(98)00093-9.

63. Hosono, M., Arai, H., Aizawa, M., Yamamoto, I., Shimizu, K., & Sugiyama, M. (1993). Decoloration and degradation of azo dye in aqueous solution supersaturated with oxygen by irradiation of high-energy electron beams. *Appl. Radiat. Isot.*, *44*(9), 1199–1203. https://doi.org/10.1016/0969-8043(93)90064-H.

64. Suzuki, N., Miyata, T., Sakumoto, A., Hashimoto, S., & Kawakami, W. (1978). The degradation of an azo dye in aqueous solutions by high-intensity electron-beam irradiation. *Int. J. Appl. Radiat. Isot.*, *29*(2), 103–108. https://doi.org/10.1016/0020-708X(78)90031-5.

65. Lee, C. S., Londhe, K., Grdanovska, S., Cooper, C. A., & Venkatesan, A. K. (2023). Emerging investigator series: low doses of electron beam irradiation effectively degrade 1,4-dioxane in water within a few seconds. *Environ. Sci.-Water Res. Technol.*, *9*(9), 2226–2237. https://doi.org/10.1039/D3EW00111C.

66. Paul, J., Rawat, K. P., Sarma, K. S. S., & Sabharwal, S. (2011). Decoloration and degradation of reactive Red-120 dye by electron beam irradiation in aqueous solution. *Appl. Radiat. Isot.*, *69*(7), 982–987. https://doi.org/10.1016/j.apradiso.2011.03.009.